

Contactless Readout of Passive LC Sensors with Compensation Circuit for Distance-Independent Measurements [†]

Marco Bau^{*}, Marco Demori, Marco Ferrari and Vittorio Ferrari

Department of Information Engineering, University of Brescia, 25123 Brescia, Italy; marco.demori@unibs.it (M.D.); marco.ferrari@unibs.it (M.F.); vittorio.ferrari@unibs.it (V.F.)

^{*} Correspondence: marco.bau@unibs.it; Tel.: +39-030-371-5896

[†] Presented at the Eurosensors 2018 Conference, Graz, Austria, 9–12 September 2018.

Published: 3 December 2018

Abstract: Contactless readout of passive LC sensors composed of a capacitance sensor connected to a coil can be performed through an electromagnetically coupled readout coil set at distance d . Resonant frequency f_s and Q-factor Q_s of the LC sensor can be extracted from the measurement of the impedance at the readout coil by using a technique theoretically independent of d . This work investigates the effects on the measurement accuracy due to the unavoidable parasitic capacitance C_P in parallel to the readout coil, which makes the measured values of f_s and Q_s dependent on d . Numerical analysis and experimental tests confirm such dependence. To overcome this limitation, a novel electronic circuit topology for the compensation of C_P is proposed. The experimental results on assembled prototypes show that for a LC sensor with $f_s \approx 5.48$ MHz a variation of less than 200 ppm across an interrogation distance between 2 and 18 mm is achieved with the proposed compensation circuit.

Keywords: distance-independent contactless readout; LC resonant sensors; telemetric sensors

1. Introduction

Passive LC sensors can be obtained by connecting a capacitive sensor to a coil, thus forming a resonant LC circuit where the measurement information is related to the resonant frequency and the quality factor of the LC circuit. By magnetically coupling the coil connected to the sensor to an external interrogation coil, contactless readout of the LC-sensor can be achieved [1]. This configuration has recently gained particular interest in several fields such as industrial, chemical or biomedical applications. The lack of wired connection to the sensor is attractive in applications where cabled solutions are difficult or unpractical, such as measurement in sealed environments or inside animal/human bodies [1,2]. Additionally, these applications can take advantage on the absence of on-board power supply, allowing in principle for unattended unlimited operation. In-field measurement conditions are typically characterized by uncontrolled distance between the readout and the sensor coils, thus requiring interrogation techniques that desirably are independent of the distance between the coils. Approaches theoretically independent of the distance have been proposed both in the time-domain [3,4] and in the frequency-domain [2]. In the latter case, measuring the real part of the impedance at the readout coil allows to obtain the resonant frequency and the quality factor of the LC sensor [5,6]. The present work investigates on the limitations of such technique when considering unavoidable parasitic capacitances in parallel to the readout coil due to the connected electronics and cables. By means of numerical simulations and experimental tests, it

has been demonstrated that the parasitic capacitances introduce dependence on the distance. As a solution, a circuit is proposed to compensate for this unwanted effect.

2. Operating Principle

Figure 1a shows the schematic diagram of the proposed contactless readout system for capacitive sensors. It is composed of the interrogation unit made up by an impedance analyzer and the readout coil represented by inductance L_1 and series resistance R_1 . The capacitance C_P models the parasitic elements coming from the windings of the coil, cables, and any electronic circuits connected in parallel to the readout coil. The readout coil is magnetically coupled to the secondary coil represented by inductance L_2 and series resistance R_2 . The magnetic coupling is described through the coupling factor $k = \pm M/(L_1L_2)^{1/2}$, where the mutual inductance M is a parameter dependent on the interrogation distance d between the two coils, their geometries and orientation. The secondary coil and the connected capacitive sensor C_S form a resonant LC circuit with resonant frequency f_s and quality factor Q_s given by:

$$f_s = \frac{1}{\sqrt{L_2C_S}}, Q_s = \frac{1}{R_2} \sqrt{\frac{L_2}{C_S}} \quad (1)$$

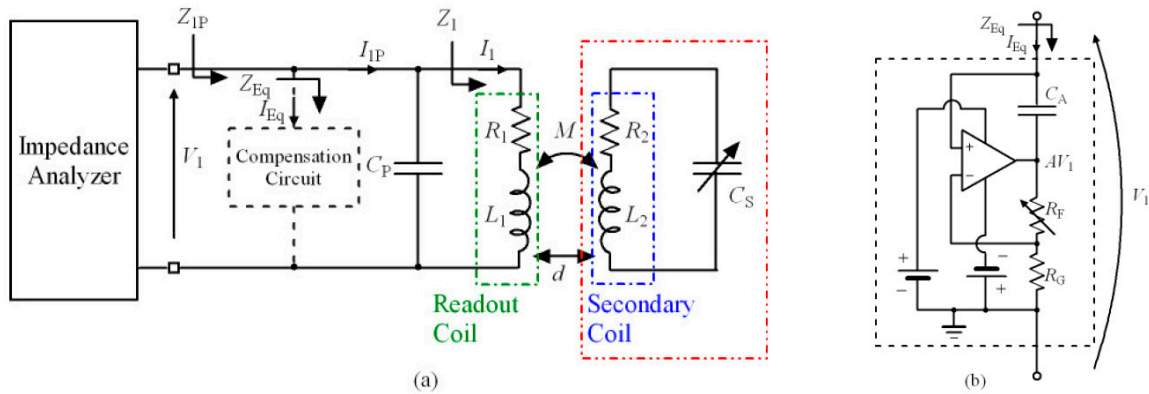


Figure 1. (a) Schematic diagram of the contactless readout system. (b) Capacitance compensation circuit.

In particular, when $C_P = 0$ and without the compensation circuit, the sensor parameters f_s and Q_s can in principle be measured by considering the real part $\text{Re}\{Z_1\}$ of the equivalent impedance $Z_1 = V_1/I_1$ through the readout coil, which results:

$$\text{Re}\{Z_1\} = R_1 + 2\pi f_s L_1 k^2 Q_s \frac{(f/f_s)^2}{1 + Q_s^2 \left(\frac{f}{f_s} - \frac{f_s}{f}\right)^2} \quad (2)$$

From (2) it can be seen that k acts only as a scaling factor and both f_s and Q_s can be derived considering the frequency f_m of the maximum of $\text{Re}\{Z_1\}$ and the Full Width at Half Maximum (FWHM) bandwidth Δf_m through the following relations [2]:

$$f_m = \frac{2Q_s}{\sqrt{4Q_s^2 - 2}} f_s, Q_s \approx \frac{f_s}{\Delta f_m} \quad (3)$$

From (3) it can be observed that for sufficiently large values of Q_s , it results $f_m \approx f_s$, obtaining a relative deviation $(f_m - f_s)/f_s < 100$ ppm for $Q_s > 50$. When $C_P \neq 0$ again, and without considering the compensation circuit, the real part of the impedance $Z_{1P} = V_1/I_{1P} = Z_1//Z_{CP}$ has the following more complex expression:

$$\text{Re}\{Z_{1P}\} = \frac{\text{Re}\{Z_1\}}{(2\pi f C_P \text{Re}\{Z_1\})^2 + (1 - 2\pi f C_P \text{Im}\{Z_1\})^2} \quad (4)$$

From (3) and (4) it can be seen that now k does not act only as a scaling factor and without knowing its value in advance, it is not possible to extract f_s and Q_s .

An analysis of the effects of k and C_P on $\text{Re}\{Z_{1P}\}$ has been performed numerically. Figure 2a shows $\text{Re}\{Z_{1P}\}$ against f/f_s , i.e., the frequency normalized to f_s , for three different values of k when $C_P/C_S=0.5$. The two vertical dotted lines are for $f/f_s = 1$, i.e., corresponding to the resonant frequency of the LC sensor, and for $f/f_s = f_P/f_s$, i.e., corresponding to the secondary resonant frequency $f_P = 1/(2\pi\sqrt{L_1C_P})$ due to L_1 resonating with C_P . When $C_P \neq 0$, two peaks are present in $\text{Re}\{Z_{1P}\}$. Denoting with f_{mP}/f_s the position of the maxima close to $f/f_s = 1$ and with f_{eP}/f_s those close to f_P/f_s , it can be observed that for decreasing values of k , f_{mP}/f_s moves towards 1 and the associated peak value decreases, while f_{eP}/f_s tends to f_P/f_s and the associated peak value increases, proving the distance-dependent behavior. For $k = 0$ there is no coupling between the readout coil and the sensor coil, and in that case, the height of the peak close to $f/f_s = 1$ vanishes and only the peak at f_P/f_s can be measured. Figure 2b shows the effect of different values of C_P/C_S at fixed $k = 0.2$. From the results, it can be noticed that for increasing C_P/C_S , the ratio f_{mP}/f_s moves towards values lower than 1, while the ratio f_{eP}/f_s tends to 1.

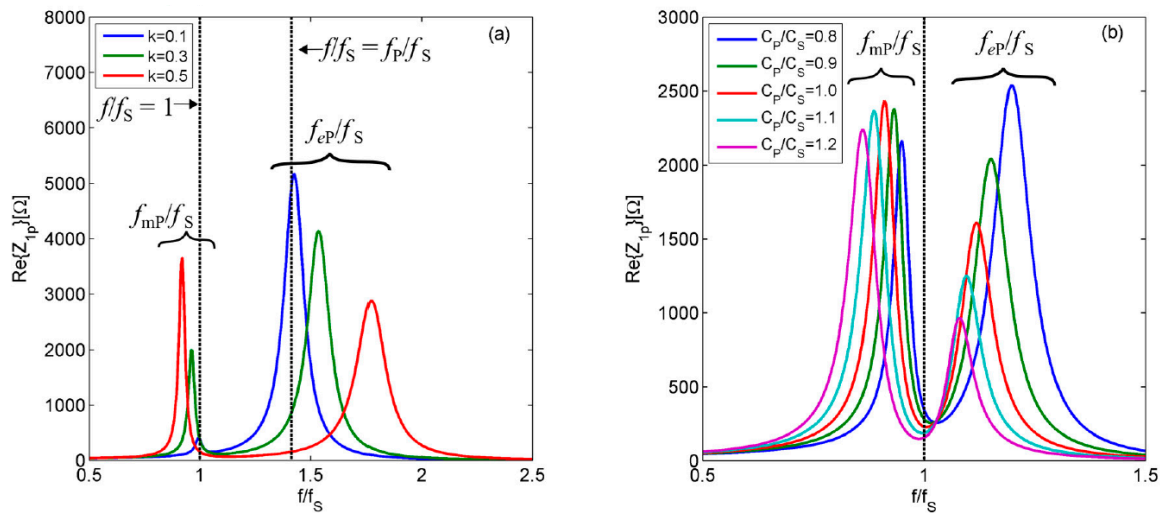


Figure 2. (a) $\text{Re}\{Z_{1P}\}$ versus the normalized frequency f/f_s for different values of k and for $C_P/C_S=0.5$. (b) $\text{Re}\{Z_{1P}\}$ versus the normalized frequency f/f_s for different values of C_P/C_S and for $k = 0.2$.

To avoid the dependence of f_{mP} on C_P and hence on the distance, the proposed compensation circuit of Figure 1b is connected in parallel to the readout coil. The circuit operates as a Negative Impedance Converter (NIC) providing the equivalent impedance $Z_{Eq} = V_i/I_{Eq} = 1/(j2\pi f(-C_C))$, where the negative capacitance $-C_C = -C_A R_F/R_G$ can be tuned through R_F to compensate and possibly cancel C_P .

3. Circuit Prototype and Experimental Results

The compensation circuit of Figure 1b has been built by using a high-bandwidth operational amplifier (AD8045). Figure 3a shows the prototype and the experimental setup adopted to validate the proposed technique. The measured equivalent parameters for the readout and sensor coils are $L_1 = 8.17 \mu\text{H}$ and $R_1 = 3.12 \Omega$, and $L_2 = 8.50 \mu\text{H}$ and $R_2 = 3.20 \Omega$ respectively. For the capacitive sensor, a capacitance $C_S = 99 \text{ pF}$ has been adopted which from (1) gives for the LC resonant circuit $f_s = 5.48 \text{ MHz}$ and $Q_s = 91.5$.

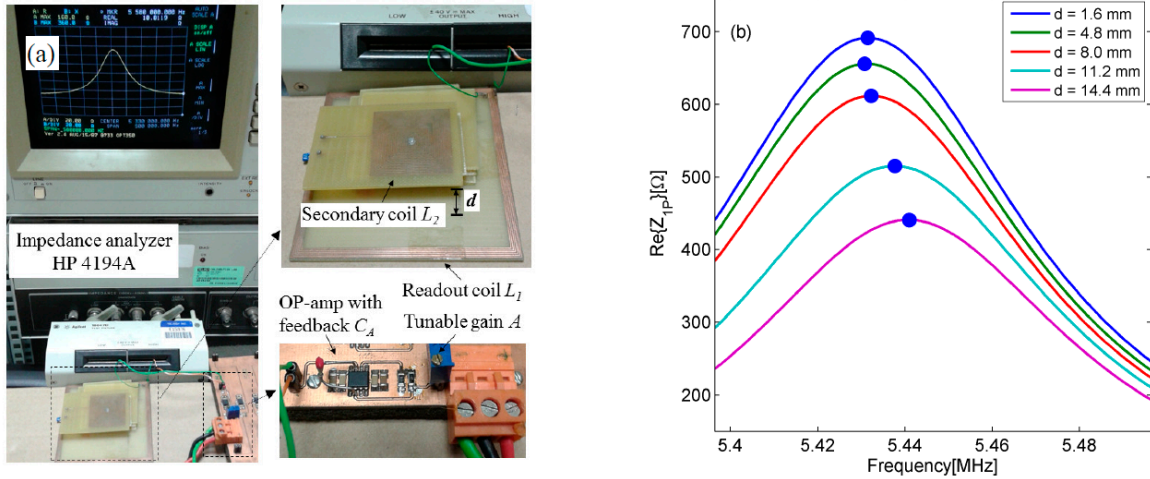


Figure 3. (a) Pictures of the experimental setup. (b) $\text{Re}\{Z_{1P}\}$ measured near f_s for different values of the interrogation distance d considering a parasitic capacitance $C_P = 47$ pF and without the compensation circuit applied.

To validate the numerical analysis of Section 2, Figure 3b shows the measured $\text{Re}\{Z_{1P}\}$ around f_s at five different distances when a total parasitic capacitance of $C_P = 47$ pF is present. It can be observed that, in agreement with the predictions of Figure 2a, the frequency of the maximum of $\text{Re}\{Z_{1P}\}$ shifts towards higher frequencies for increasing distances, i.e., for decreasing values of k . Figure 4a shows the results of the same test with the compensation circuit tuned for the cancellation of C_P activated. Figure 4b compares the cases of Figures 3b and 4a, showing the relative frequency deviation $\Delta f/f = 10^6(f_{mP} - f_s)/f_s$ as a function of the estimated coupling factor k . With the compensation circuit connected, a maximum relative deviation $\Delta f/f$ less than 200 ppm is achieved.

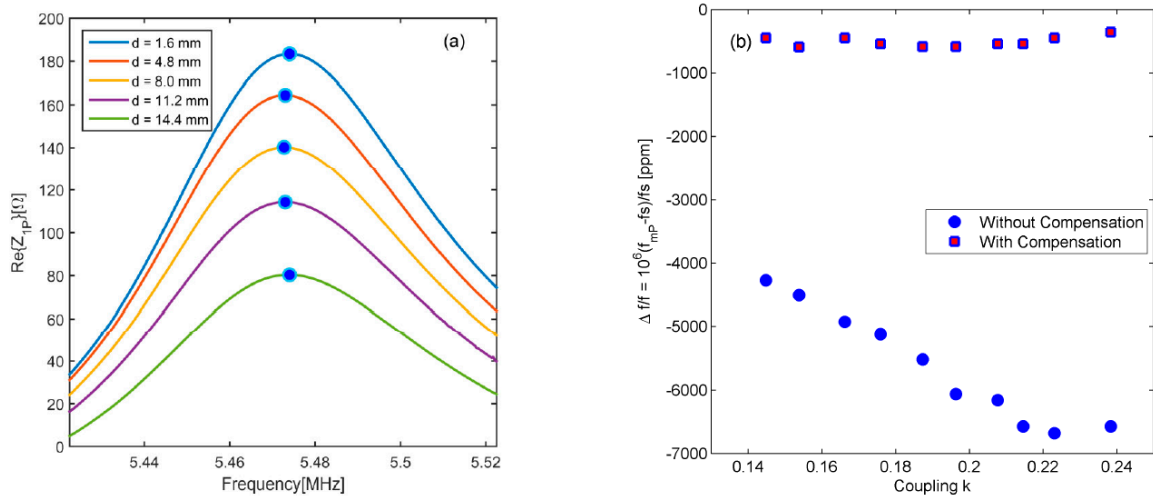


Figure 4. (a) $\text{Re}\{Z_{1P}\}$ measured near f_s for different values of the interrogation distance d considering a parasitic capacitance $C_P = 47$ pF with the compensation circuit applied. (b) Comparison of the relative frequency deviation $\Delta f/f = 10^6(f_{mP} - f_s)/f_s$ with and without the compensation circuit applied.

4. Conclusions

The effect of a parasitic capacitance in parallel to the readout coil for contactless measurement of LC passive sensors has been investigated. Numerical analyses and experimental tests show that the parasitic capacitance introduces a dependence of the measured resonant frequency on the interrogation distance. A capacitance compensation circuit is proposed and validated to counteract the effect of the parasitic capacitance, outperforming equivalent systems based on the impedance phase-dip measurement proposed in the literature.

References

1. Huang, Q.A.; Dong, L.; Wang, L.F. LC Passive Wireless Sensors Toward a Wireless Sensing Platform: Status, Prospects, and Challenges. *J. Microelectromech. Syst.* **2016**, *25*, 822–840, doi:10.1109/JMEMS.2016.2602298.
2. Nopper, R.; Niekrawietz, R.; Reindl, L. Wireless Readout of Passive LC Sensors. *IEEE Trans. Instrum. Meas.* **2010**, *59*, 2450–2457, doi:10.1109/TIM.2009.2032966.
3. Demori, M.; Masud, M.; Baù, M.; Ferrari, M.; Ferrari, V. Passive LC sensor label with distance-independent contactless interrogation. In Proceedings of the 16th IEEE SENSORS Conference, Glasgow, UK, 30 October–1 November 2017; doi:10.1109/ICSENS.2017.8234410.
4. Ferrari, M.; Baù, M.; Tonoli, E.; Ferrari, V. Piezoelectric resonant sensors with contactless interrogation for mass-sensitive and acoustic-load detection. *Sensors and Actuators, A: Physical* **2013**, *202*, 100–105, doi:10.1016/j.sna.2013.04.029.
5. Demori, M.; Baù, M.; Ferrari, M.; Ferrari, V. Electronic Technique and Circuit Topology for Accurate Distance-Independent Contactless Readout of Passive LC Sensors. *Int. J. Electron. Commun. (AEÜ)* **2018**, *92*, 82–85, doi:10.1016/j.aeue.2018.05.019.
6. Demori, M.; Baù, M.; Ferrari, M.; Ferrari, V. Interrogation techniques and interface circuits for coil-coupled passive sensors. *Micromachines* **2018**, *9*, 449, doi:10.3390/mi9090449.



© 2018 by the authors. Licensee MDPI, Basel, Switzerland. This article is an open access article distributed under the terms and conditions of the Creative Commons Attribution (CC BY) license (<http://creativecommons.org/licenses/by/4.0/>).